Scientific Journal of Impact Factor (SJIF): 4.72

e-ISSN : 2348-4470
p-ISSN : 2348-6406

International Journal of Advance Engineering and Research Development

National Conference On Nanomaterials, (NCN-2017)

Volume 4, Special Issue 6, Dec.-2017 (UGC Approved)

Hybrid PVA-In_2O_3 Nano Thin Film for Transparent Optical Devices

Sathish Sugumaran [1*#], Dinesh Muthu[2], Chandar Shekar Bellan[1*], Dinesh Bheeman[3] and Sharmila Chandran[4]

[1] *Nanotechnology Research Lab, Department of Physics, Kongunadu Arts and Science College, G-N Mills, Coimbatore- 641 029, Tamil Nadu, India.*
[2] *Department of Physics, Bharathiar University, Coimbatore, 641 046, Tamil Nadu, India.*
[3] *Biology Division, Department of Applied Sciences, Higher College of Technology, Muscat, 133 Sultanate of Oman.*
[4] *Department of Physics, PSGR Krishnammal College for Women, Coimbatore- 641 004, Tamil Nadu, India.*

[#] *Present address: Institute for Solid State Physics (ISSP), Division of Nanoscale Science, University of Tokyo, 5-1-5 Kashiwanoha, Chiba Japan 277-8581.*

Abstract:- *Hybrid PVA-In_2O_3 transparent nano thin film (293 nm) was prepared by very simple and cost effective dip coating method. The effect of annealing temperature on the functional group, structure, morphology and optical properties was investigated. The presence of metal-oxide (In-O) bond was confirmed from Fourier transform infrared spectroscopy. X-ray diffraction patterns revealed the predominantly amorphous in nature of the films. Scanning electron microscopy images revealed spherical shaped uniform grains distributed over the entire film surface. The sizes of the grains increased with increase of annealing temperature. The percentage of transmittance (80 to 90%) increases whereas band gap energy (3.80 to 3.76 eV) values decreases with increase of annealing temperature. The obtained results indicated that the amorphous nature and high transmittance with wide band gap of the prepared transparent hybrid nano thin films indicated the feasibility of utilizing these nano thin films in transparent optical device applications.*

Keywords: *PVA, In_2O_3, structure, morphology and optical properties.*

Introduction

Hybrid/composite thin films are a fascinating research for the scientist around the globe. Among hybrid materials, the polymer and inorganic oxide based thin films attracted the attention of researchers mainly because of their interesting physical and chemical properties [1-4]. It offers great prospects for the most efficient and cost effective utilization of a wide variety of applications. In particular, PVA (poly (vinyl alcohol)) is a vital role in hybrid film form due to potential role against thermal, environmental degradation, good chemical resistance and easy film forming by simple methods [5, 6]. Additionally, PVA's ability to dissolve in water, transparency over the entire visible spectrum and good adhesion to glass substrate makes it to be used in various fields and in the production of mechanically strong hybrids. For commercial applications, PVA is selected because its properties still appear to be unique in terms of the price/performance ratio [7]. New technologies are demanding PVA materials with improved structure, morphology, electrical and optical modifications of traditional PVA for the development of nano devices. To further enhance the properties of this polymer, an inorganic material is added to PVA to form a hybrid, which could be lightweight, flexible and exhibit a good moldability [8-10]. To the best of our knowledge, there is no report on effect of annealing on structure, morphology and optical properties of hybrid PVA-In_2O_3 thin films by dip coating method. This study explores the preparation of as-grown and annealing effect on hybrid PVA-In_2O_3 thin films for transparent optical device applications.

2. Experimental Techniques

2.1. Preparation

The PVA and In_2O_3 powders were purchased from Sigma Aldrich and NICE Chemical Pvt. Ltd, Cochin, India. Initially, PVA solution was prepared by adding 0.5g of PVA powder in 50 ml of distilled water and this mixture was magnetically stirred at 85^oC for 5h. Then 0.5 g of In_2O_3 powder is added to PVA solution and stirred for 2h followed by repeated ultrasonication until homogeneous dispersion of PVA- In_2O_3 solution was got. Precleaned glass substrates were dipped into the homogeneously dispersed PVA- In_2O_3 solution for deposition of hybrid thin films by dip coating method. The schematic diagram of hybrid thin film is shown in Fig. 1.

2.2. Characterization

The functional groups present in the films were identified by Thermo Nicolet, Avatar 370 Fourier transform infrared spectroscopy (FTIR) with a spectral range of 4000-400 cm $^{-1}$ and resolution of 4 cm $^{-1}$. The structural properties were characterized by X-ray diffraction (XRD) using Bruker AXS D8 advance diffractometer with Cukα radiation (λ= 1.5406 A^{o}) with operating voltage 40 kV and a current of 30 mA. The surface morphology of the film was imaged using JEOL Model JSM - 6390LV scanning electron microscope (SEM). The elemental compositional of the films were analyzed with JEOL Model JED – 2300 energy dispersive X-ray analysis (EDS). The optical transmission spectrum of the films was analyzed using JASCO 670 UV-Vis-NIR spectrophotometer for the wavelength range of 200-2500 cm^{-1}.

3. Results and Discussion

3.1. Functional group analysis

Fig. 2 shows the FTIR of as grown and annealed hybrid PVA-In_2O_3 thin films. A relatively broad absorption stretching band is observed at 3423-3432 cm^{-1} indicating the presence of polymeric association of the free hydroxyl groups and bonded OH stretching vibrations [11]. A broad O-H absorption stretching vibration is observed at 3423-3432cm^{-1} due to the result from the superposition of multiple polymeric H bonds associated with the crystalline phase and dimeric H bonds associated with the amorphous phase [12]. As the film is subjected to annealing at 50°C, 100°C and 150°C the intensity of the absorption band reduces with increase of annealing temperature. The observed reduction in the intensity of the absorption band with annealing temperature indicated that the water content in the film is removed when the film is subjected to annealing temperature and the reduction the water contents is more effective for above 100°C annealing temperature. Anti-symmetric $\gamma_{as}(CH_2)$ and symmetric $\gamma_s(CH_2)$ stretching bands of CH_2 groups observed at between 2900 and 2934 cm^{-1}.

The bands at around 1632-1634 cm^{-1} is due to OH bending. The symmetric bending mode $\gamma_{\delta}(CH_2)$ is found at between 1427 and 1442 cm^{-1}. The wide overlapping bands between 1054 and 1300 cm^{-1} may results from the superposing effect of In-O, In-O-C, C-O-C and it is a difficult to distinguish between them. The spectrum seems to be consistent with that previously reported work in literature [12-14]. The observed very weak peak at around 600 cm^{-1} may be attributed to In-OH mode [15]. The several peaks obtained between 400 cm^{-1} and 800 cm^{-1} is due to metal-oxide (possibility of In-O vibrations) bond [16]. The obtained M-O bond is in good agreement with previously reported work on metal oxide thin film in polymer matrix [12]**.** This results manifested the conclusion about the specific interaction in hybrid polymer matrices and hence the complexation. Thus, complex formation in the hybrid polymer matrices has been confirmed from this analysis [17]. The clear observation from the IR spectra, it is observed that some of the additional peaks and some of them were disappeared with respect to the reported work on virgin PVA thin films [18, 19**].**

3.2. Structure analysis

The XRD patterns of as grown and annealed PVA- In_2O_3 hybrid thin films are shown in the Fig. 3. PVA is well known as a crystalline polymer due to the strong intermolecular interaction between PVA chains through intermolecular hydrogen bonding [12]. The XRD patterns revealed a broad pattern (characteristics of small particle size) at 2θ=20-38^{o} was obtained for both as grown and for films subjected to annealing at 50˚C, 100˚C, 150˚C [20]. The diffraction phase around 2θ =9, 25 and 55˚ corresponding to PVA crystalline phase [21], whereas Bragg's reflection at 22, 30, 36, 51 and 61^{o} corresponding to (211), (222), (400), (440) and (622) of cubic phase of In_2O_3 [22].

The complexation of PVA chains with In_2O_3 would lead to a decrease in the intermolecular interaction between the PVA chains and thus the crystalline degree. This was well proved by the decrease in the diffraction intensity from the crystalline PVA. Similar work has been reported in literature for PVA based hybrid thin film [23]. The observed a large peak that demonstrates the major nanostructure of the films, while small narrow peaks are a proof for minor microcrystalline in the film matrix. It is seen that the intensity of the diffraction peak increases with increase of annealing temperature [24]. The absence of any intense peaks throughout the spectrum for PVA-In_2O_3 hybrid thin films indicated the predominantly amorphous nature of the film [18, 25]. The XRD pattern implies that the film has a less ordered structure, i.e., amorphous in nature. The heat treatment during preparation was limited to 150˚C to avoid the degradation of PVA thus resulting in immature calcinations leading to less crystalline film i.e. close to amorphous in nature.

3.3. Morphological analysis

The morphological analysis of the PVA-In_2O_3 hybrid thin films were illustrated in fig 4. The SEM figures showed that the In_2O_3 powders arranged in a spherical shape with uniformly distributed over the entire film surface. Annealed films showed aggression of In_2O_3 particles with regularly arranged in spherical shape [26]. All the prepared films showed average grain size of 269 nm to 561 nm with more homogenous manner [15]. The observed size of grains was 269-275 nm for as grown film whereas aggregated with grain sizes of 325-380 nm, 350-425 nm and 347- 561nm for annealed at 50^{o}C, 100^{o}C and 150^{o}C films respectively [27, 28]. Hence it is clear that, when the annealing temperature increases, the size of grain undergoes agglomerates to form bigger sized grains.

The observed increase of grain size with increase of annealing temperature is good in agreement with early reported work in the literature [29, 30]. The surface morphology clearly shows that as grown and annealed hybrid PVA-In_2O_3 films are homogeneous and fine dispersion of In_2O_3 particle in the polymer matrix. Similar morphology is observed for various polymer/inorganic hybrid thin films reported in literature [31,32]. SEM images revealed that the hybrid PVA-In_2O_3 films are homogenous, uniform distribution of particles and spherical shape with different grain sizes of the prepared hybrid thin films are potential candidate for optoelectronic applications [33].

3.4. Elemental analysis

Elemental analysis obtained from EDS of PVA-In_2O_3 hybrid thin films is shown in Fig. 5. The spectrum indicates that the observed intensity corresponding In and O for both as grown and annealed thin films. Further increasing annealing temperature affects the intensity of the elements. The spectrum confirms that the elements of In and O are present in the both as grown and annealed films. The atomic percentage with elements of indium is rich as compare to oxide for both as grown and annealed hybrid thin films. From this graph it is seen that the presence of indium at 3.5 eV and oxide at 0.5 eV.

3.5. Optical study

The optical transmittance spectra of as grown and annealed PVA/In_2O_3 hybrid thin film is shown in Fig. 6. The as grown film shown transmittance about 80 %, whereas annealed films at 50˚C, 100˚C, 150˚C showed a 10% increment in transmittance value. The as grown film showed transmittances about 80% at lower wavelength range and it increase to about 85% at higher wavelength region. The transmittance was found to be increasing up to 90 % with increase of annealing temperatures. It is seen that the transmittance values are increases with increase of annealing temperature. The observed trend of transmittance with annealing temperature is in good agreement with early reported work in literature [34]. The increase in transmittance with increase in annealing temperature leads to reduction in the surface diffusion and voids [35]. It clearly indicates that the increase in annealing temperature leads to improvement of surface smoothness and decrease in thickness, grain boundary scattering, rms surface roughness [36]. This is a prime cause for increase in transmittance upon increase in annealing temperature.

The optical band gap energy of hybrid thin films was estimated by extrapolating the linear portion of the curves resulting from Tauc's plot (Fig. 7). The determined band gap energy is 3.80 eV for as grown and annealed at 50^{o}C film whereas 3.79 eV for annealed at 100^{o}C and 3.76 eV for film annealed at 150 ^{o}C. It is clearly shows that the band gap energy values are decreases with increase of annealing temperature. This may be due to increase in grain size, decrease in number of defects and low oxygen content [37].

The determined band gap energy value of as grown film is good in agreement with early reported work on PVA-In_2O_3 hybrid thin films [12]. The similar effect of annealing temperature on the bandgap energy values on various hybrid thin films reported in literature [38]. The obtained higher transmittances with wide band gap energy value are essential for the prepared thin film for transparent optical device applications.

Conclusion

A simple and cost effective dip coating method was used to prepare transparent PVA-In_2O_3 hybrid thin films. The FTIR spectrum indicated the presence of metal complexes of indium and oxide in the PVA polymer matrix. Stretching vibration of M-O bond occurs and this confirms the formation of In_2O_3 nanoparticles in the polymer matrix. The presence of elements such as In and O are in the films were confirmed from EDS. The absence of any intense peaks throughout the XRD patterns indicated the predominantly amorphous nature of the film. Heat treatment during preparation was limited to 150˚C to avoid the degradation of PVA thus resulting in immature calcinations leading to less crystalline film i.e. close to amorphous in nature showing weak Bragg's refection. SEM images revealed that the spherical shaped of In_2O_3 nanoparticles are uniformly distributed over the entire film surface. The optical analysis showed the transmittance values are increases with increase of annealing temperature whereas band gap energy values are decreases with increase of annealing temperature. The obtained smooth surface, amorphous nature and high transmittance (90%) with wide band gap energy (3.76 -3.80 eV) of hybrid thin film could be used in transparent optical device applications.

References

[1] H.L. Tai, Y.D. Jiang and G. Z. Xie, *J. Electron. Sci. Technol.* 8, 154 (2010).
[2] N. Bouropoulos, G.C. Psarras, N. Moustakas, A. Chrissanthopoulos and S. Baskoutas, *Phys. Status Solidi (a)* 8, 2033 (2008).
[3] S. Sugumaran, C.S. Bellan and M. Nadimuthu, *Int. J. Polym. Anal. Charact.*19, 549 (2014).
[4] L.Wang, M.H. Yoon, Y. Yang, A. Facchetti and T.J. Marks, *Nat. Mater.* 5, 893 (2006).
[5] S. Sathish and B. Chandar Shekar, Transparent nano composite thin films for thin film

transistors & opto-electronic devices, Applications of Nano Materials: Electronics, Energy and Environment, Bloomsbury Publishing Pvt. Ltd, ISBN: 978-93-82563-35-8, (2012), pp. 289-296.
[6] J.S. Park J.W. Park and E. Ruckenstein, *Polymer* 42, 4271 (2001).
[7] S. Sugumaran and C. S. Bellan, *Optik* 125, 5128 (2014).
[8] S. H. S. Zein, A. R. Boccaccini and W.N.H.W. Zainal, *World Appl. Sci. J.* 6, 737 (2009).
[9] S. Sathish, B. Chandar Shekar and N. Manivannan, *Iran. Polym. J.* 24, 63 (2015).
[10] S. Sugumaran, C.S. Bellan, D. Muthu,S. Raja,D. Bheeman and R. Rajamani, *Polym. Adv. Technol.* 26, 1486 (2015).
[11] M.Tsukada,G.Fereddi and J.S.Grighton, *J. Polym. Sci. B: Polym. Phys.* 32, 243 (1994).
[12] S. Sathish, M. Dinesh and B. Chandar Shekar, *Int. J. Adv. Mater. Sci.* 4, 93 (2013).
[13] B.V.K. Naidu, M. Sairam, K.V.S.N. Raju and T.M. Aminabhavi, *J. Appl. Polym. Sci.* 260, 142 (2005).
[14] L. Damliac and C. David, *Polymer* 37, 5219 (1996).
[15] H. Tai, Y. Jiang, G. Xie and J. Yu, *J. Mater. Sci. Technol.* 26, 605 (2010).
[16]. E.C.C. Souza, J.F.Q. Rey and E.N.S. Muccillo, *Appl. Surf. Sci.* 255, 3779 (2009).
[17] P.K. Khanna, N. Singh and S. Charan, *Mater. Lett.* 61, 4725 (2007).
[18] B. Chandar Shekar, S. Sathish and R.Sathyamoorthy, *Int. J. Nanotechnol. Appl.* 5, 297 (2011).
[19] A. M. Shehap, *Egypt J. Solids* 31, 75 (2008).
[20] X.D. Ma, X.F. Qian, J.Yin and Z.K. Zhu, *J. Mater. Chem.* 12, 663 (2002).
[21] P.D. Hong, J.H. Chen and H.L. Wu, *J. Appl. Polym. Sci.* 69, 2477 (1998).
[22] A.Z. Sadek, W. Wlodarski, K. Shin, R.B. Kaner and K. Kalantar-zadeh, *Nanotechnol.* 17, 4488 (2006).
[23] D.Saikia, P.K. Saikia, P.K. Gogoi and P. Saikia, *Dig. J. Nanomater. Bios.* 6, 589 (2011).
[24] M.H. Habibi and N. Talebian, *Acta Chim. Slov.* 52, 53 (2005).
[25] S. Sathish, B. Chandar Shekar and R. Sathyamoorthy, *Physics Procedia* 49, 160 (2013).
[26] A. Chatterjee, C.H. Shen, A.Ganguly, L.C.Chen, C.W. Hsu, J.Y. Hwang and K.H. Chen, *Chem. Phys. Lett.* 391, 278 (2004).
[27] M. Hashizume and T. Kunitake, *RIKEN Review* 38, 36 (2001).
[28] A. Mitsionis, T. Vaimakis, C. Trapalis, N. Todorova, D. Bahnemann and R. Dillert, *Appl. Catal. B: Environ.* 106, 398 (2011).
[29] N. Yahya, M.N. Akhtar, A.F. Masuri and M. Kashif, *J. Appl. Sci.* 11, 1303 (2011).
[30] P.E. Agbo and M.N. Nnabuchi, *Chalcogenide Lett.* 8, 273 (2011).
[31] A. Lagashetty, V. Havanoor, S. Basavaraja and A. Venkataraman, *Bull. Mater. Sci.* 28, 477 (2005).
[32] J.P. Borah and K.C. Sarma, *Acta Phys. Pol.* 114, 713 (2008).
[33] K.J. Loh and D. Chang, *J. Mater. Sci.* 46, 228 (2011).
[34] B. Barman and K.C. Sarma, *Chacogenide Lett.* 8, 171 (2011).
[35] S. Sathish, B. Chandar Shekar, S. Chandru Kannan, R. Sengodan, K.P.B. Dinesh and R. Ranjithkumar, *Int. J. Polym. Anal. Charact.* 20, 29 (2015).
[36] S. Sugumaran, C S. Bellan and D. Bheeman, *Opt. Mater.* 72, 618 (2017).
[37] S. Sugumaran, M. N. Ahmad, M. F. Jamlos, C.S. Bellan, S. Pattiyappan, R. Rajamani R. Sivaraman, *Opt. Mater.* 49, 348 (2015).
[38] S. Sugumaran, C.S. Bellan, D, Muthu, S. Raja, D. Bheeman and R. Rajamani, *RSC Adv.* 5, 10599 (2015).

Figure Captions

Fig.1 Schematic diagram of hybrid PVA-In_2O_3 thin film
Fig. 2 FTIR spectra of as grown and annealed hybrid PVA-In_2O_3 thin films
Fig 3 XRD patterns of as grown and annealed hybrid PVA-In_2O_3 thin films
Fig. 4 SEM image of as grown and annealed hybrid PVA-In_2O_3 thin films
Fig. 5 EDS spectra of as grown and annealed hybrid PVA-In_2O_3 films
Fig. 6 UV-Vis transmittance spectra of as grown and annealed hybrid PVA-In_2O_3 films
Fig. 7 Tauc's plot- $(\alpha h\nu)^2$ versus hν of hybrid PVA-In_2O_3 films

Hybrid PVA-In_2O_3 Nano Thin Film for Transparent Optical Devices

Sathish Sugumaran [1*#], Dinesh Muthu[2], Chandar Shekar Bellan[1*], Dinesh Bheeman[3] and Sharmila Chandran[4]

Fig. 1

Hybrid PVA-In_2O_3 Nano Thin Film for Transparent Optical Devices

Sathish Sugumaran [1*#], Dinesh Muthu[2], Chandar Shekar Bellan[1*], Dinesh Bheeman[3] and Sharmila Chandran[4]

Fig. 2

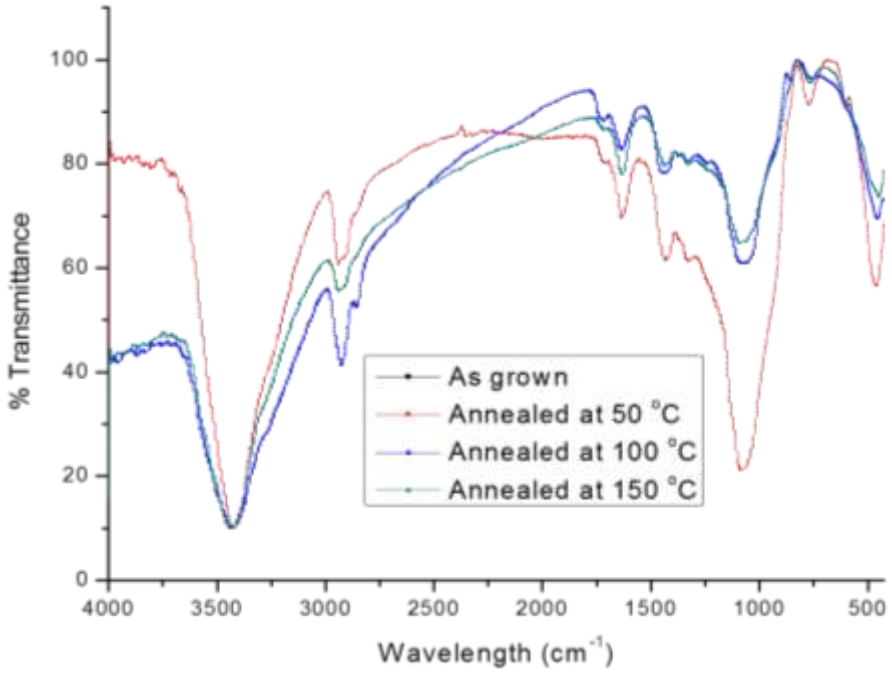

Hybrid PVA-In_2O_3 Nano Thin Film for Transparent Optical Devices

Sathish Sugumaran [1*#], Dinesh Muthu[2], Chandar Shekar Bellan[1*], Dinesh Bheeman[3] and Sharmila Chandran[4]

Fig. 3

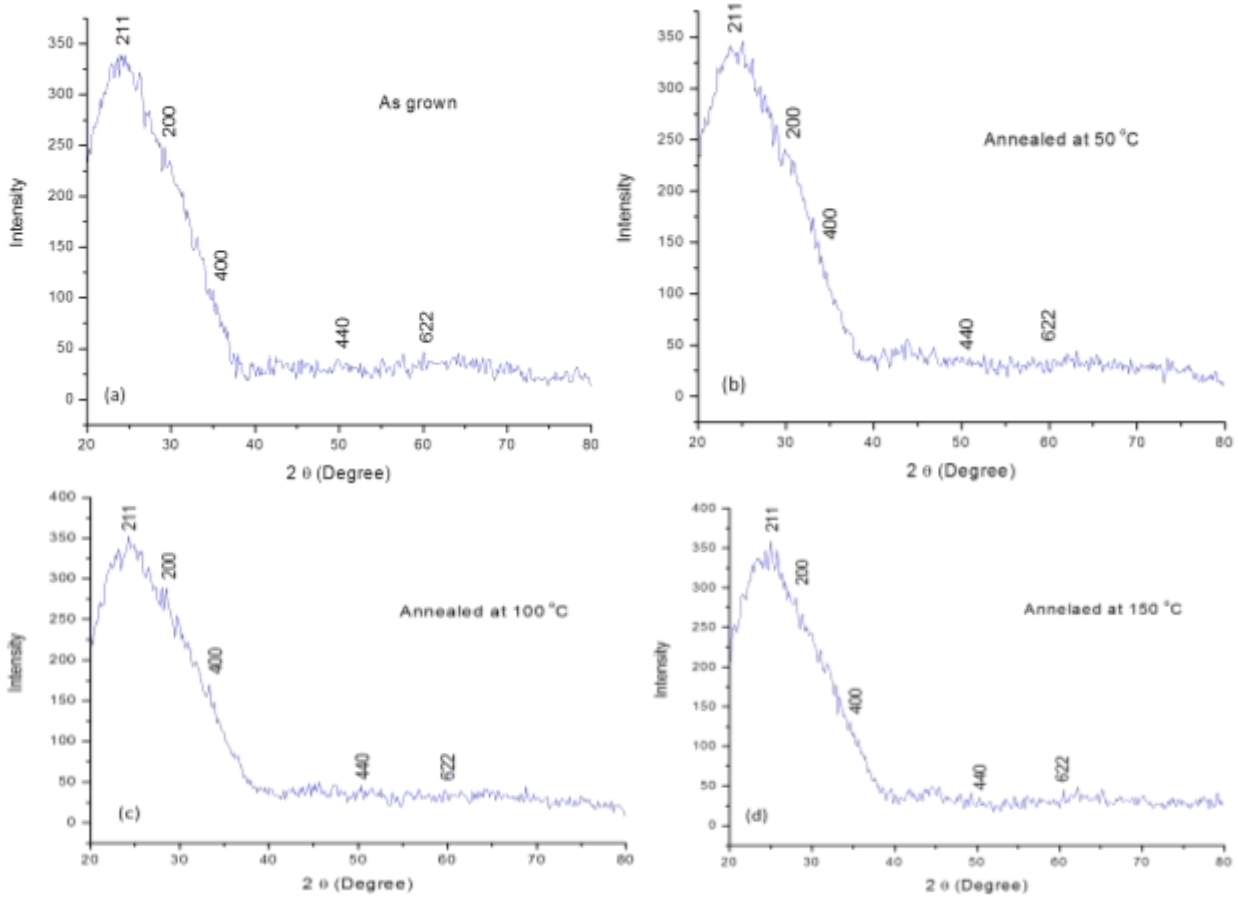

Hybrid PVA-In_2O_3 Nano Thin Film for Transparent Optical Devices

Sathish Sugumaran [1*#], Dinesh Muthu[2], Chandar Shekar Bellan[1*], Dinesh Bheeman[3] and Sharmila Chandran[4]

Fig. 4

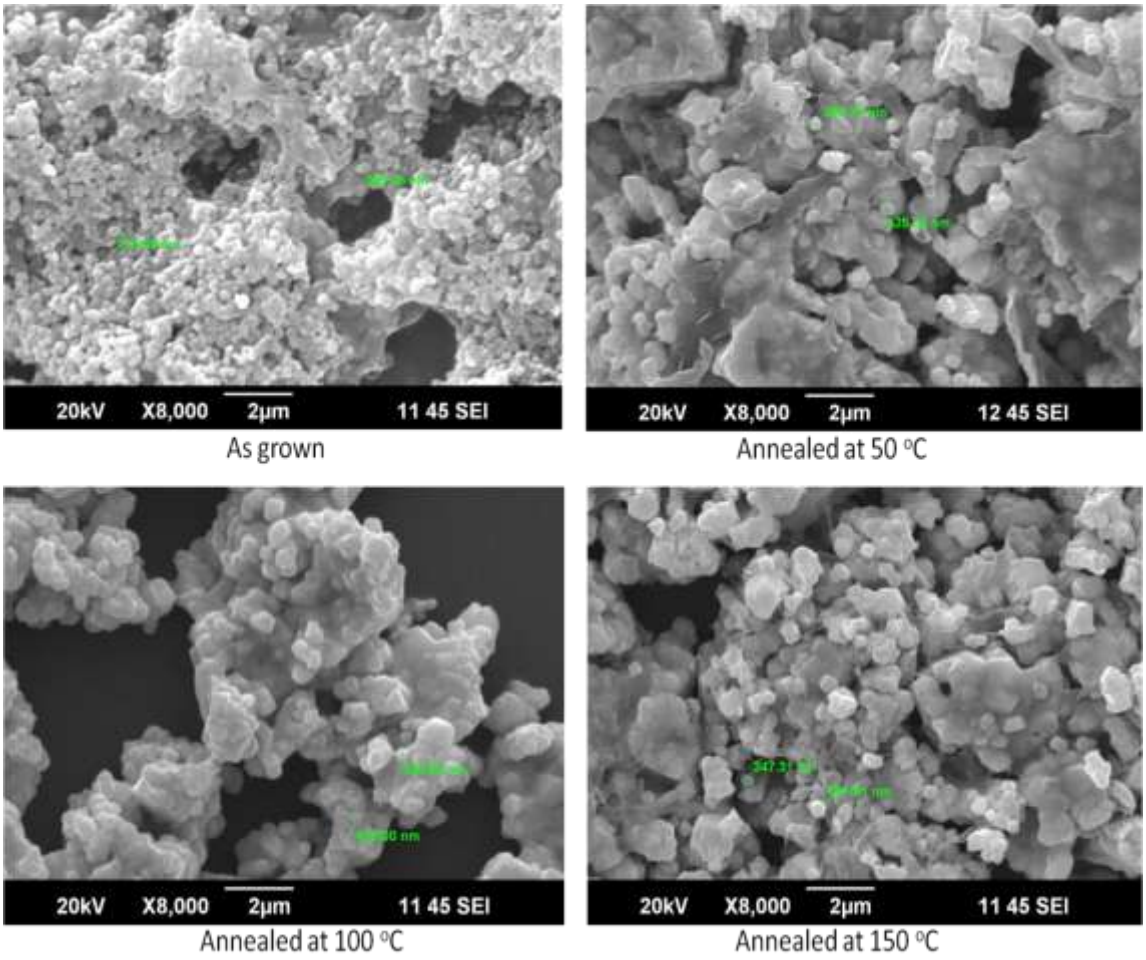

Hybrid PVA-In_2O_3 Nano Thin Film for Transparent Optical Devices

Sathish Sugumaran [1*#], Dinesh Muthu[2], Chandar Shekar Bellan[1*], Dinesh Bheeman[3] and Sharmila Chandran[4]

Fig. 5

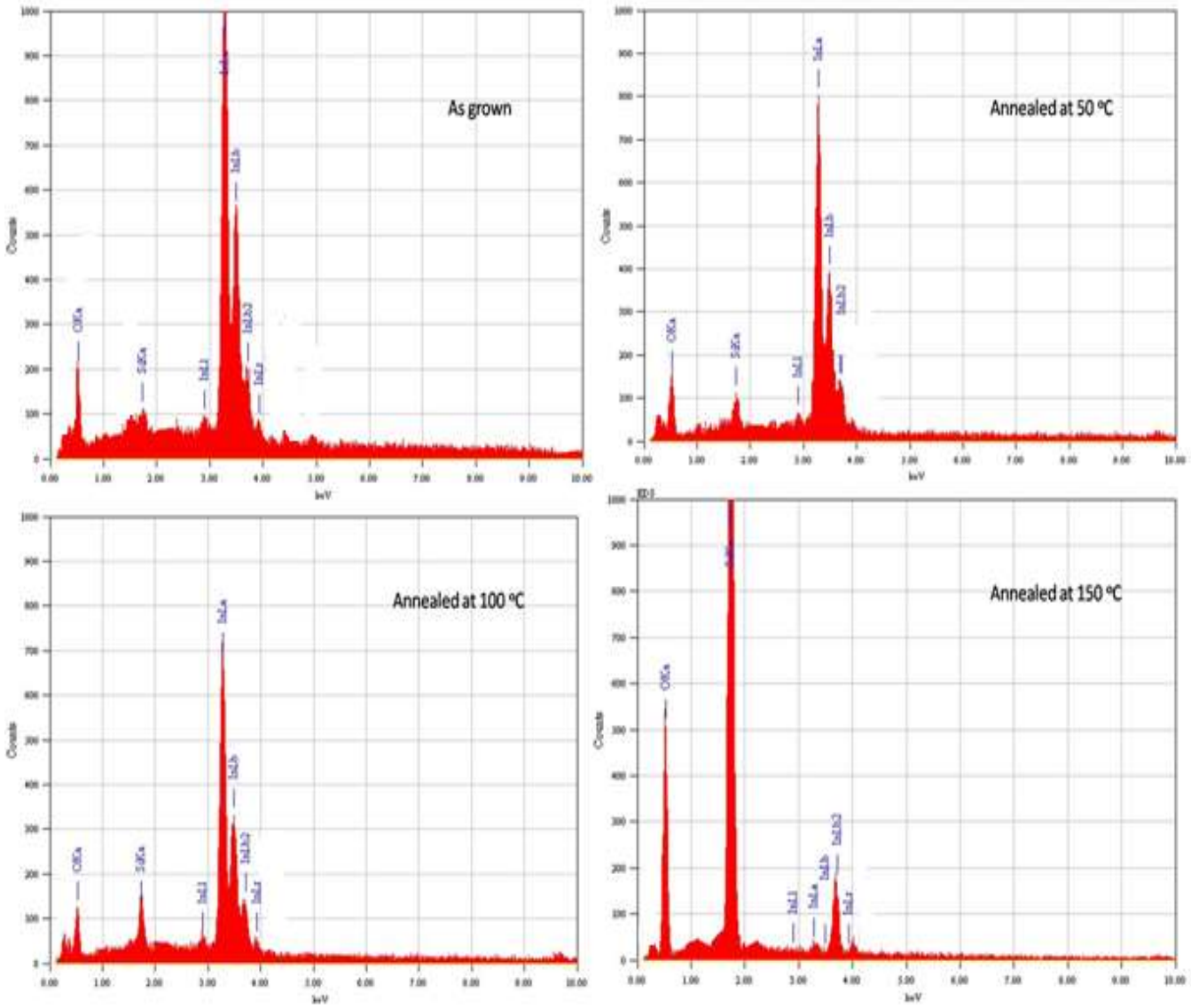

Hybrid PVA-In_2O_3 Nano Thin Film for Transparent Optical Devices

Sathish Sugumaran [1*#], Dinesh Muthu[2], Chandar Shekar Bellan[1*], Dinesh Bheeman[3] and Sharmila Chandran[4]

Fig. 6

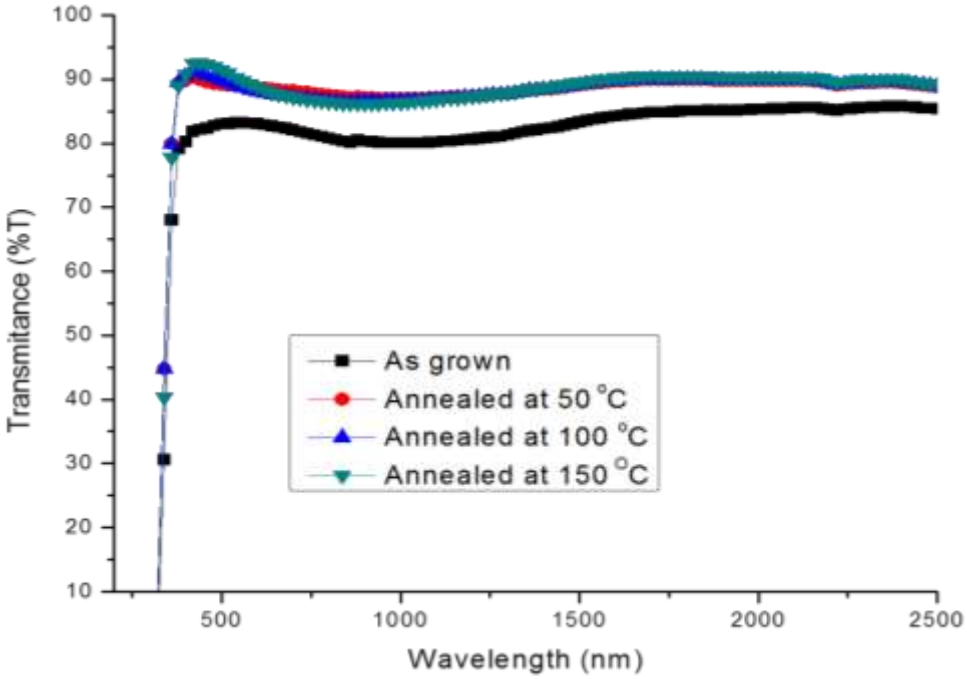

Hybrid PVA-In_2O_3 Nano Thin Film for Transparent Optical Devices

Sathish Sugumaran [1*#], Dinesh Muthu[2], Chandar Shekar Bellan[1*], Dinesh Bheeman[3] and Sharmila Chandran[4]

Fig. 7